Supporting Information

Significant inhibition of secondary pollution in the catalytic oxidation of chloroaromatics over a bifunctional Ru_1/CeO_2 single-atom catalyst

Yu Wang[‡,a], Zhang Liu[‡,c], Yao Wei[‡,d,e], Yiming Hu[f], Yi Chen[a,f], Bin Shan*[c] and Bo Wu*[b,g]

[a] College of Resources and Environment Engineering, Wuhan University of Science and Technology, Wuhan 430081, P. R. China

[b] CAS Key Laboratory of Low-Carbon Conversion Science and Engineering, Shanghai Advanced Research Institute, Chinese Academy of Sciences, Shanghai 201210, P. R. China. wubo0422@ustc.edu.cn

[c] State Key Laboratory of Materials Processing and Die and Mould Technology, School of Materials Science and Engineering, Huazhong University of Science and Technology, Wuhan, 430074, P. R. China. bshan@mail.hust.edu.cn

[d] Shanghai Institute of Applied Physics, Chinese Academy of Sciences, Shanghai 201204, P. R. China

[e] University of Chinese Academy of Sciences, Beijing 100049, P. R. China

[f] Tongxiang Ties Environmental Energy co., Ltd., Jiaxing 314500, P. R. China

[g] Hefei National Laboratory for Physical Sciences at the Microscale, University of Science and Technology of China, Hefei, Anhui 230026, P. R. China
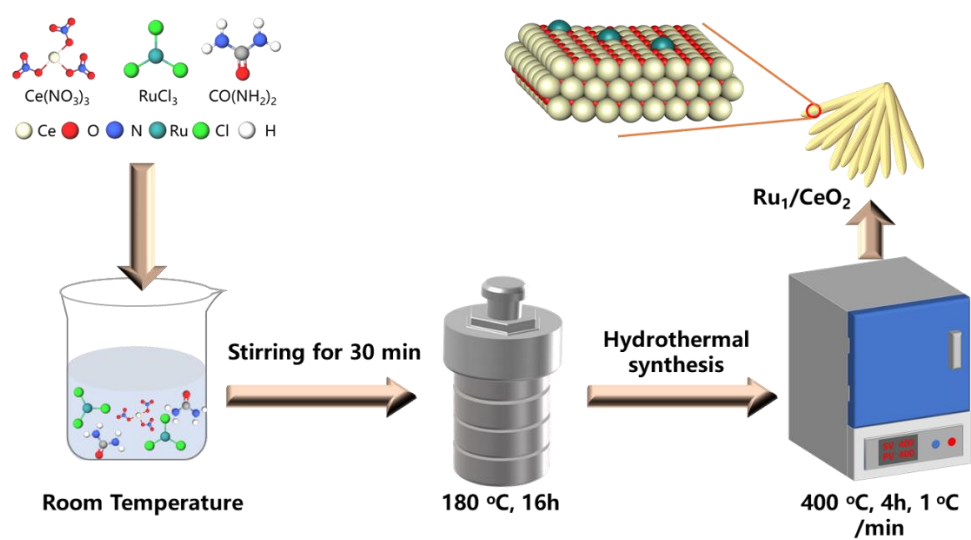
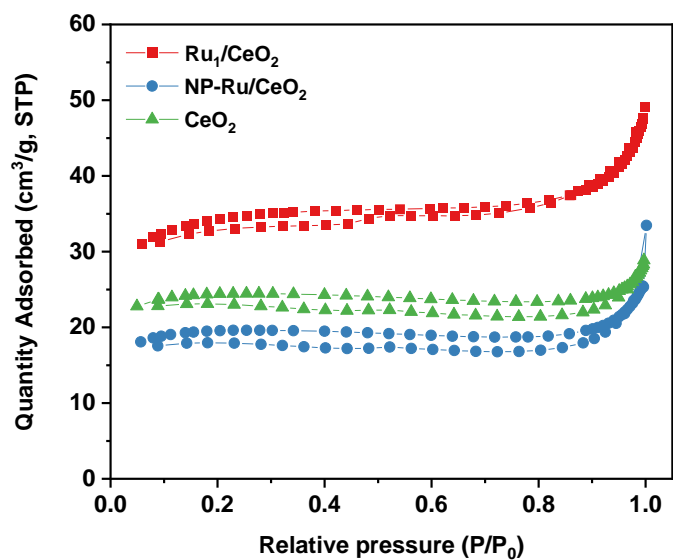**Figure S1.** Schematic illustrations of the preparation of Ru_1/CeO_2 catalyst.

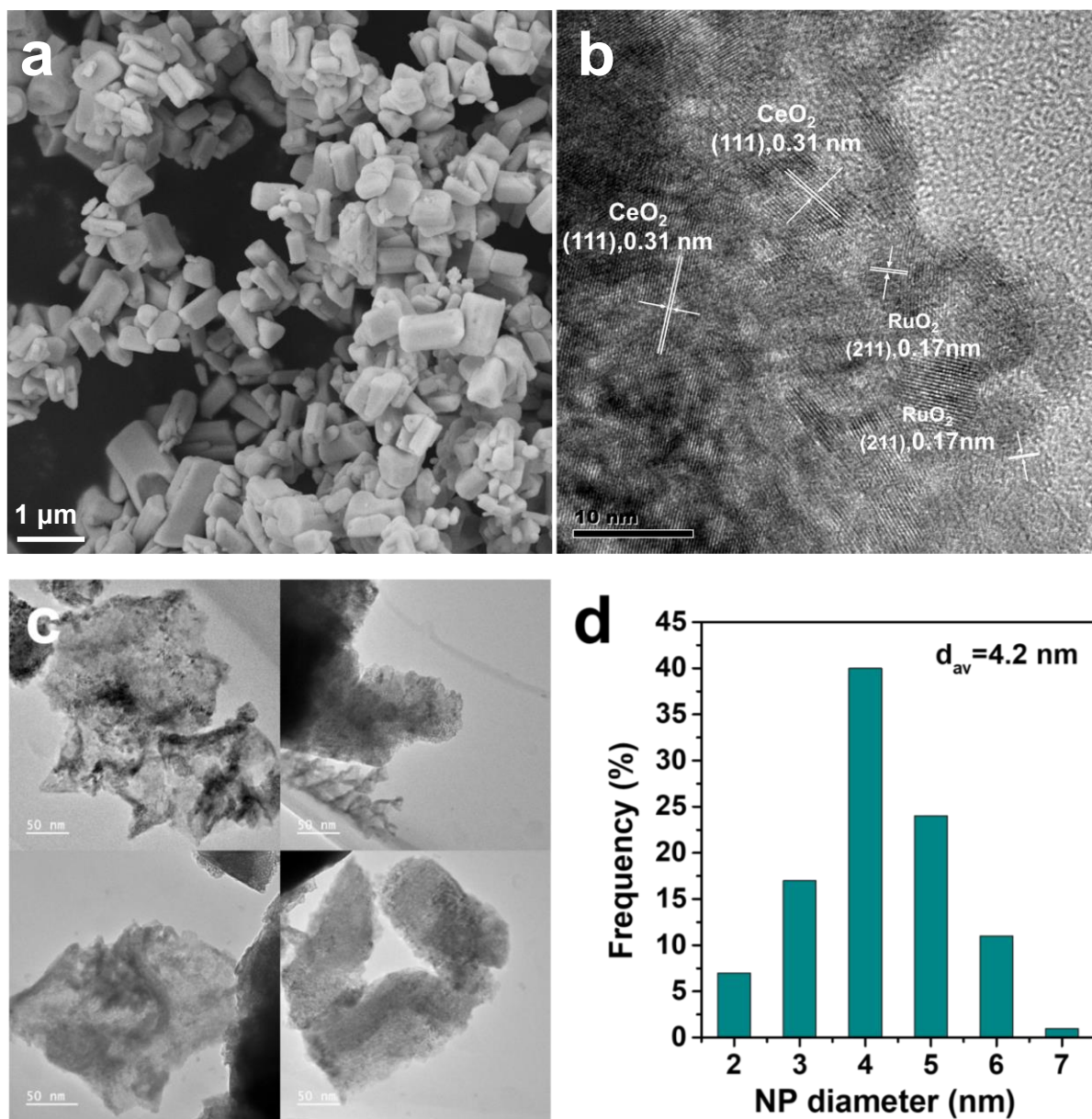**Figure S2.** N_2 adsorption-desorption isothermal of CeO_2, Ru_1/CeO_2 and NP-Ru/CeO_2.

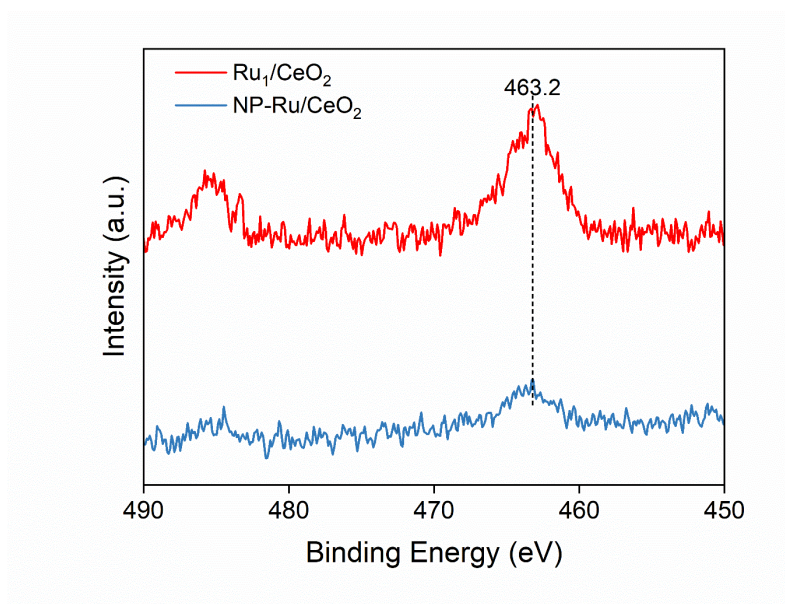**Figure S3.** (a) SEM, (b) HRTEM, (c) TEM images and (d) histogram of RuO_2 NPs particle size for $NP-Ru/CeO_2$.
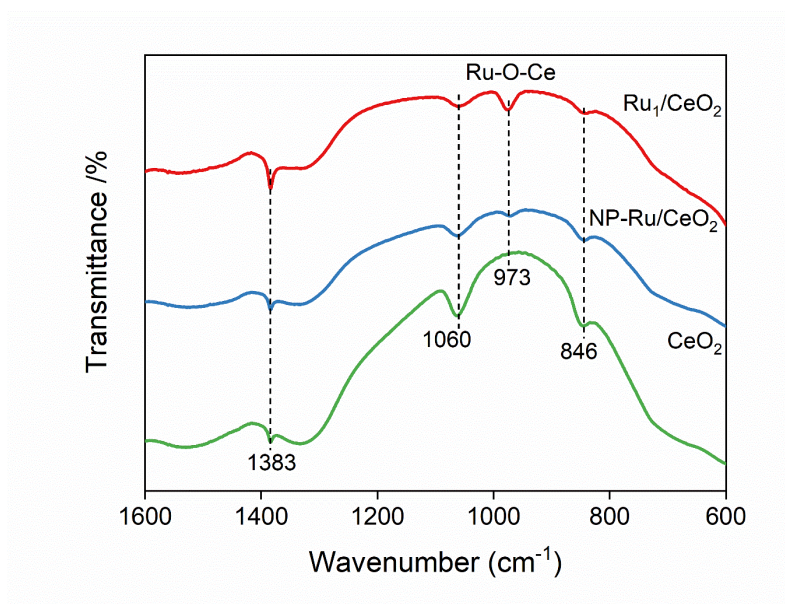
Figure S4. Ru 2p spectra of Ru_1/CeO_2 and $NP-Ru/CeO_2$.

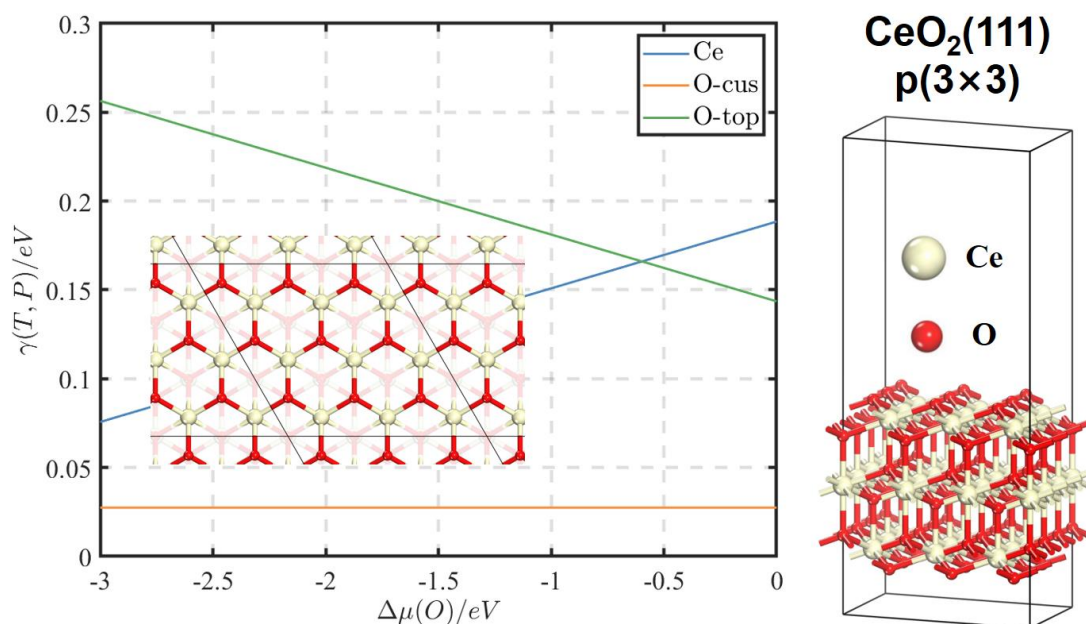**Figure S5**. FTIR spectrum for CeO_2, Ru_1/CeO_2, and $NP\text{-}Ru/CeO_2$.

Figure S6. O chemical potential calculation showed that $CeO_2(111)$ exposed the O-cus to seal under experimental conditions. a $CeO_2(111)$ p(3×3) slab model was established with 9 layers of atoms, 3 layers under fixed, and a 15 Å vacuum layer.

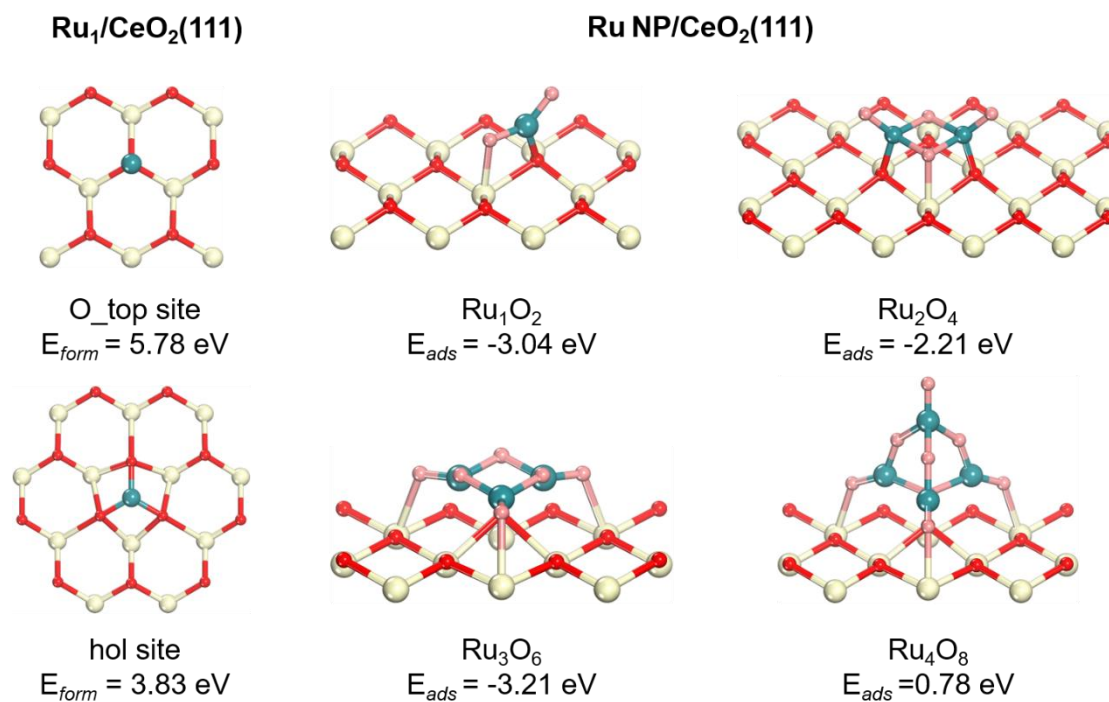**Figure S7.** Ru atoms tend to bind to the hollow site formed by 3 O atoms of $CeO_2(111)$. As for $(RuO_2)_n/CeO_2(111)$, when n=3, the configuration of the Ru_3O_6 cluster loaded by $CeO_2(111)$ is the most stable model.
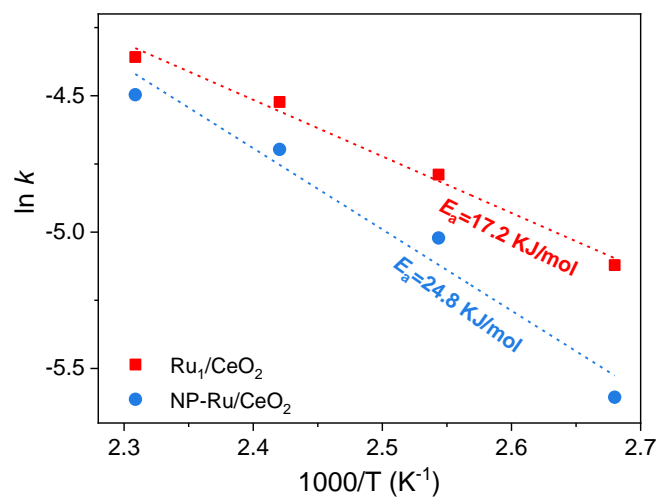
Figure S8. Arrhenius plots and apparent activation energy (E_a) of Ru_1/CeO_2 and NP-Ru/CeO_2, respectively. Reaction conditions: 1000 ppm CB/5 vol.% H_2O/air.
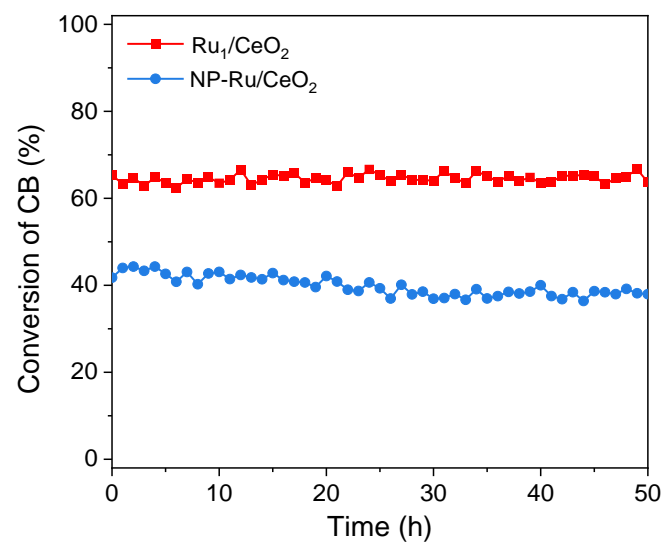
Figure S9. Long-term stability tests of CB oxidation tested at 200 °C over Ru_1/CeO_2 and
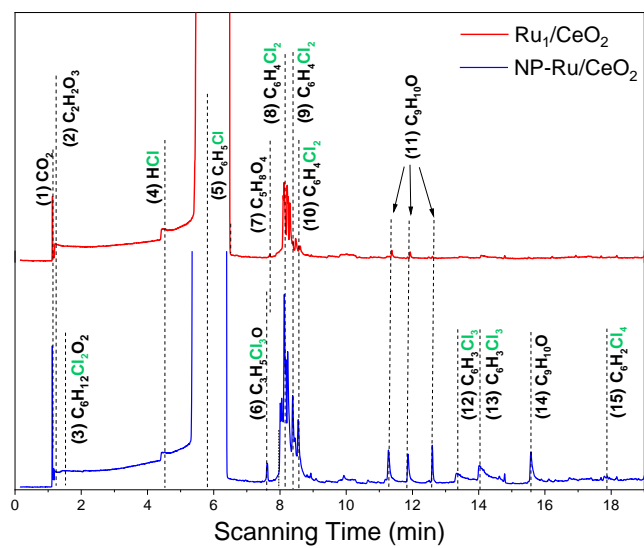
$NP\text{-}Ru/CeO_2$.

Figure S10. Possible reaction intermediate products detected by GC-MS during the CB oxidation at 240 °C over Ru_1/CeO_2 and NP-Ru/CeO2.

Table S1. ICP-OES study and physiochemical properties for all the samples.

Catalyst	Ru content (wt%) [a]	S_{BET} (m^2/g) [b]	Pore volume (cm^3/g) [b]
CeO$_2$	0	73.3	0.044
Ru$_1$/CeO$_2$	1.04	105.5	0.074
NP-Ru/CeO$_2$	1.06	58.9	0.040

[a] The Ru content was determined by ICP-OES. [b] The surface area and pore volume were measured by N$_2$ adsorption-desorption isotherm.

Table S2. Structural parameters extracted from Ru K-edge XAFS fitting.

Samples	Shell	CN[a]	R (Å)[b]	σ^2 (10^{-3} Å^2)[c]	ΔE_0 (eV)[d]	R-factor (%)[e]
Ru foil	Ru-Ru	12	2.67±0.003	3.0±0.5	4.6±0.7	0.9
RuO$_2$	Ru-O	6	1.96	/	/	/
	Ru-Ru	2	3.11	/	/	
NP-Ru/CeO$_2$	Ru-O	4.5±0.6	1.94±0.01	4.2±1.9	–3.9±1.8	2.1
	Ru-Ru	2.2±0.6	3.14±0.05	5.0±1.9	–3.9±1.8	
Ru$_1$/CeO$_2$	Ru-O	4.1±0.9	1.95±0.02	5.9±3.1	3.0±2.8	1.4
	Ru-Ru	/	/	/	/	

[a] CN, coordination number. [b] R, distance between absorber and backscatter atoms. [c] σ^2, Debye–Waller-factor to account for both thermal disorder and structural disorder. [d] ΔE_0, inner potential correction to account for the differences in the inner potential between the sample and the reference compound. [e] R-Factor (%) indicates the goodness of the fit. The obtained S_0^2 of Ru foil was 0.75 and it was fixed in the subsequent fitting of Ru foil K-edge data for the catalyst.

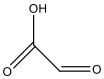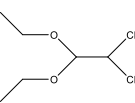**Table S3.** Surface properties for CeO_2, Ru_1/CeO_2 and $NP-Ru/CeO_2$.
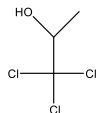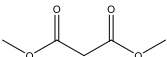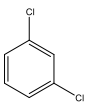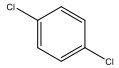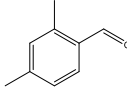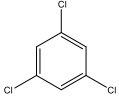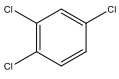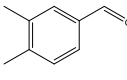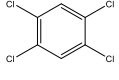
Entry	Catalyst	$O_\beta/(O_\alpha+O_\beta)$ [a]	EPR ratio [b]	I_D/IF_{2g} [c]
1	CeO_2	0.37	1	0.0145
2	Ru_1/CeO_2	0.44	1.66	0.0568
3	$NP-Ru/CeO_2$	0.67	1.99	0.0811

[a] Determined from the XPS in O 1s region. [b] Determined from the EPR spectra, we set the integrated area (in the range from 2.003-2.030) of CeO_2 as 1, the EPR ratio was calculated based on the integrated area of Ru_1/CeO_2 and $NP-Ru/CeO_2$ divide the integrated area of CeO_2. [c] Determined from Raman spectra.

Table S4. Recently reported Ru-based catalysts for CB catalytic oxidation.

Catalysts	GHSV (mL/g h) and CB Conc. (ppm)	T_{50} / T_{90} (°C)	Rate at 200 °C (mmol/(g h))	Ru content (wt.%)	TOFs at 200 °C (h^{-1})	Ref.
Ru$_1$/CeO$_2$	**30000, 1000**	**192/220**	**0.83**	**1.04**	**8.07**	**this work**
NP-Ru/CeO$_2$	**30000, 1000**	**202/227**	**0.55**	**1.06**	**5.28**	**this work**
Ru/Fe1Mn2	20000, 600	158/197	0.53	0.94	5.70	[1]
0.05P/RuCe	15000, 217	175/250	0.09	0.75	1.27	[2]
Ru/SnO$_2$	30000, 1000	280/310	0.03	1.21	0.22	[3]
1%Ru/TiO$_2$	60000, 500	275/287	0.01	1.00	0.14	[4]
Ru5/Ti-350	60000, 500	240/260	0.16	4.83	0.34	[5]
1Ru-5Ce/TiO$_2$	60000, 500	258/283	0.07	0.50	1.35	[6]
1%Ru/Ti$_5$Ce$_{95}$	12000, 550	187/224	0.20	1.15	1.73	[7]
1%Ru/SBA-15	12000, 550	312/350	0.01	1.00	0.06	[8]
Ru/CeO$_2$-r	30000, 1000	230/280	0.28	0.38	7.48	[9]
1%Ru-CeO$_2$	12000, 550	205/248	0.13	0.58	2.26	[10]
Ru/CeO$_2$	60000, 1000	250/280	0.03	0.80	0.34	[11]

Table S5. Qualitative analyses of the byproducts in the off-gases from the CB oxidation over Ru_1/CeO_2 and NP-Ru/CeO$_2$ samples.

No.	Molecular formula	Molecular structure	Compound name
1	CO_2	CO_2	carbon dioxide
2	$C_2H_2O_3$		2-oxoacetic acid
3	$C_6H_{12}Cl_2O_2$		1,1-dichloro-2,2-dimethoxyethane
4	HCl	HCl	chlorine hydride
5	C_6H_5Cl		chlorobenzene
6	$C_3H_5Cl_3O$		1,1,1-trichloropropan-2-ol
7	$C_5H_8O_4$		dimethyl malonate
8	$C_6H_4Cl_2$		1,3-dichlorobenzene
9	$C_6H_4Cl_2$		1,4-dichlorobenzene
10	$C_6H_4Cl_2$		1,2-dichlorobenzene
11	$C_9H_{10}O$		2,4-dimethylbenzaldehyde
12	$C_6H_3Cl_3$		1,3,5-trichlorobenzene
13	$C_6H_3Cl_3$		1,2,4-trichlorobenzene
14	$C_9H_{10}O$		3,4-dimethylbenzaldehyde
15	$C_6H_2Cl_4$		1,2,4,5-tetrachlorobenzene

References

1.   G. Wang, Y. Wang, L. Qin, B. Zhao, L. Guo and J. Han, *Catal. Sci. Technol.*, 2020, **10**, 7203-7216.

2.   Q. Dai, K. Shen, W. Deng, Y. Cai, J. Yan, J. Wu, L. Guo, R. Liu, X. Wang and W. Zhan, *Environ. Sci. Technol.*, 2021, **55**, 4007-4016.

3.   J. Zhao, W. Xi, C. Tu, Q. Dai and X. Wang, *Appl. Catal. B: Environ.*, 2020, **263**, 118237.

4.   X. Liu, L. Chen, T. Zhu and R. Ning, *J. Hazard. Mater.*, 2019, **363**, 90-98.

5.   J. Wang, H. Zhao, X. Liu, W. Xu, Y. Guo, J. Song and T. Zhu, *Catal. Lett.*, 2019, **149**, 2004-2014.

6.   M. Ye, L. Chen, X. Liu, W. Xu, T. Zhu and G. Chen, *Catalysts*, 2018, **8**, 116.

7.   Q. Dai, S. Bai, J. Wang, M. Li, X. Wang and G. Lu, *Appl. Catal. B: Environ.*, 2013, **142-143**, 222-233.

8.   Q. Dai, S. Bai, X. Wang and G. Lu, *Appl. Catal. B: Environ.*, 2013, **129**, 580-588.

9.   H. Huang, Q. Dai and X. Wang, *Appl. Catal. B: Environ.*, 2014, **158-159**, 96-105.

10.   Q. Dai, S. Bai, Z. Wang, X. Wang and G. Lu, *Appl. Catal. B: Environ.*, 2012, **126**, 64-75.

11.   X. Lv, M. Jiang, J. Chen, D. Yan and H. Jia, *Appl. Catal. B: Environ.*, 2022, **315**, 121592.